UC Berkeley
UC Berkeley Previously Published Works

Title

MAIDEN: a model to analyze ecosystem processes in dendroecology

Permalink

https://escholarship.org/uc/item/2sv354bb

Journal

Canadian Journal of Forest Research, 34

Author

Misson, Laurent

Publication Date

2004

Peer reviewed

MAIDEN: a model for analyzing ecosystem processes in dendroecology

Laurent Misson

Abstract: Ecophysiological and dendroecological data from a temperate sessile oak (*Quercus petraea* (Matt.) Liebl.) stand in Belgium were used to develop and parameterize a dendroecological process-based model. The purpose of this model is to serve as a tool for exploring the relationship between climate variability and tree growth based on dendroecological data. When parameterized, the model was able to correctly simulate measurements of bud-burst date, throughfall ($r^2 = 0.95$), soil water content ($r^2 = 0.81$), transpiration ($r^2 = 0.80$), and ring-width series from 1960 to 1999 ($r^2 = 0.46$). Model sensitivity analysis showed that atmospheric vapor pressure deficit is the major controlling factor of transpiration in this type of ecosystem. The model shows that bole increment is principally controlled by temperature because it affects the phenological process of bud burst and thus the growing season length. Precipitation variability does not affect variation of transpiration rate and bole increment because calculated soil water stress is negligible during the simulation period. Discrepancies between observed and simulated bole increment may be a consequence of stand density variations and worm defoliation in the spring. The MAIDEN model is particularly suited for dendreocological analysis because it takes simple species, site condition, and climatic variables as input.

Résumé : Des données écophysiologiques et dendroécologiques provenant d'un peuplement au climat tempéré de chêne sessile (*Quercus petraea* (Matt.) Liebl.), en Belgique, ont été utilisées pour développer et paramétrer un modèle dendroécologique basé sur les processus. Le rôle de ce modèle est de servir d'outil d'exploration de la relation entre la variabilité climatique et la croissance des arbres sur la base de données dendroécologiques. Une fois paramétré, le modèle est capable de simuler correctement des mesures de dates de débourrement, de précipitation non interceptée ($r^2 = 0,95$), de teneur en eau du sol ($r^2 = 0,81$), de transpiration ($r^2 = 0,80$) et des séries d'épaisseurs de cerne de 1960 à 1999 ($r^2 = 0,46$). Une analyse de sensibilité du modèle montre que le déficit de pression de vapeur d'eau est le facteur déterminant pour la transpiration dans ce type d'écosystème. Le modèle montre que la croissance du tronc est principalement contrôlée par la température, parce que celle-ci affecte le processus phénologique du débourrement et par là même la longueur de la saison de croissance. La variabilité de la précipitation n'affecte pas la variation du taux de transpiration et la croissance du tronc parce que le stress hydrique calculé est négligeable pendant la période de simulation. Des divergences entre les accroissements observés et simulés du tronc peuvent être la conséquence des variations de la densité du peuplement et des défoliations printanières. Le modèle MAIDEN est particulièrement adapté à l'analyse dendroécologique parce qu'il requiert des intrants simples tels l'espèce, les paramètres de condition de station et les variables climatiques.

[Traduit par la Rédaction]

Introduction

Understanding the relationship between climate and tree growth is critical to evaluate the vulnerability of forests to environmental changes. In addition, analyzing the interaction between forest ecosystems and the carbon cycle is essential to quantify how much carbon dioxide these ecosystems can absorb, thus helping to mitigate climate change (Woodward and Smith 2001).

L. Misson.[1] Université catholique de Louvain, Unité des eaux et forêts, Place Croix du Sud, 2 boîte 9, 1348 Louvain-la-Neuve, Belgique.

[1]Present address: Department of Environmental Science, Policy and Management, 151 Hilgard Hall, University of California Berkeley, Berkeley, CA 94720-3110, USA (e-mail: lmisson@nature.berkeley.edu).

The interactions between the vegetation and the atmosphere depend upon complex and nonlinear relationships. Consequently, they can only be understood, predicted, and extrapolated in time and space using process-based models. Several projects have produced data at high resolution that have made it possible to develop, parameterize, and validate biophysical models capable of treating the effects of short-term weather variations on energy, carbon, and water fluxes at stand level (e.g., Law et al. 2000*a*, 2000*b*; Baldocchi and Meyers 1998; Williams et al. 1996). Difficulties arise when upscaling to longer time and larger spatial scales. For long-term applications, which can include various species and habitats, other data collecting and modeling approaches are needed (Mäkelä and Hari 1986; Running and Coughlan 1988; Hunt et al. 1991; Berninger and Nikinmaa 1997).

For several decades now, dendroecology has provided efficient tools for evaluating variations in forest environments on long-time intervals and large spatial scales over different species and habitats (Fritts and Swetnam 1989). Among other applications, dendroecological studies have been useful in producing information on forest decline (e.g., LeBlanc

and Foster 1992), effects of global changes on forest ecosystems (e.g., Rathgeber et al. 2000), and forest management (e.g., Misson et al. 2003). Nevertheless, the data collecting approach does not allow an in-depth process-oriented data analysis. Tree-ring series are usually modeled using purely statistical tools, and the results are often very empirical (Cook and Kairiukstis 1990). Process-based models are more explanatory, since they offer a detailed description of ecophysiological processes. So, the development of new process-based models for use in dendroecology is likely to advance our understanding of the ecophysiological reasons for variations in tree ring width (Vaganov 1996; Rathgeber et al. 2000; LeBlanc and Terrell 2001).

This paper describes an innovative approach that tries to fill the gap in previous and ongoing studies by combining data collection, analysis, and modeling on various time and spatial scales. The MAIDEN model (modeling and analysis in dendroecology) was developed as an exploratory tool that would allow an in-depth process-oriented analysis of the relationship between climate and tree growth based on dendroecological data. This model had to work for various species and habitats as well as for different climates and site conditions. During the first stage of this research, we used fine-resolution ecophysiological data to develop and parameterize a process-based model of ring-width data. The data came from an experimental sessile oak stand (*Quercus petraea* (Matt.) Liebl.) located in the temperate climate of Belgium. During the second stage, rougher resolution dendroecological data were used to test the model in various ecological conditions. These data came from 21 Aleppo pine stands (*Pinus halepensis* Mill.) in the Mediterranean climate of southeastern France. This paper presents the general methodology of our research and the results of the first stage. A second paper will deal with the comparison of trees functioning in different ecosystems (Misson et al. 2004).

Material and methods

Data

General description

The experimental stand is located in Chimay, Belgium (50°06′N, 04°16′E), at an altitude of 260 m, in the temperate climate of the medio-European phytosociological domain. This site is part of the intensive monitoring programme (level II) of the ICP (International Co-operative Programme on Assessment and Monitoring of Air Pollution Effects on Forests) forests network, and detailed ecophysiological and dendroecological data were available. The mean annual temperature is 8.5 °C, and annual precipitation is 1002 mm (1954–2000 period). The stand is a 0.74-ha coppice with standards, with sessile oak (*Quercus petraea* (Matt.) Liebl.) as the dominant species and hornbeam (*Carpinus betulus* L.) in the understorey. Ground vegetation is dominated by *Rubus* sp. In 2002, the oak trees were 116 years old, and the hornbeam was around 20 years old. Mean circumference and dominant height of oaks were, respectively, 170 cm and 23.7 m in winter 2000. The soil is clayey (clay ≅ 50%, sand ≅ 5%) and is 1.5 m deep. It is classified as a Dystric Cambisol (FAO class).

Water cycle

From May to December 2001, throughfall was estimated using stemflow collectors on five hornbeam trees as well as four automatic rain gauges installed in the understorey at 1.3 m above the ground. Stemflow collectors were not installed on oaks because water collected is negligible for this species. The proportion of hornbeam stemflow to total throughfall was 3.1% (June to November 2001). Three piezometers were installed at 100 cm depth to study the time course of the groundwater table. From May to December 2001, the groundwater table did not reach the piezometers. Volumetric soil water contents were measured every 15 min using 12 time domain reflectometry probes (CS615, Campbell Scientific Ltd., Loughborough, UK) installed at different depths (10, 20, 40, 70, and 100 cm) inside three pedological pits.

Sap flux density (F_d, kg·m^{-2}·h^{-1}) was monitored from May to November 2001. We used the Granier thermal method with 2 cm long radial sapflow meters. Each sensor had two probes, one was heated continuously at a constant power and the other was not heated. The two probes were installed vertically 15 cm apart, on the northern side of trees to avoid direct solar heating. The system was shielded with aluminum foil to minimize temperature fluctuations in the sapwood. This method was applied on five oaks with basal areas covering the range of basal area classes of the stand. The mean circumference of these trees was 179.3 cm in winter 2001. The sap flux at tree level (F, kg·h^{-1}) was calculated by the relation $F = F_d S$, where S is the tree sapwood area (m^2). This area was measured on stained cores extracted with a Pressler auger. A conducting wood area at 1.3 m proved to be an excellent scalar of flux at stand level (Hatton et al. 2000). Upscaling from tree to stand was then based on the estimation of the stand sapwood area.

Canopy cover

In 1997, 1998, and 2000, the respective dates of bud burst and leaf fall were estimated using a standard European methodology (Preushler 1994). From 1996 to 2001, leaf area index (LAI, one-sided green leaf area per unit ground area) was estimated directly by collecting litterfall four times a year by means of ten 0.5-m^2 litter traps placed 1 m above the ground level. Specific leaf area (SLA, leaf area per unit mass) was measured on 100 randomly selected leaves for each species. SLA was 0.016 m^2·g^{-1} for oak and 0.024 m^2·g^{-1} for hornbeam. Comparable values were reported in another study in a similar environment (C. Vincke, personal communication). From May to November 2001, LAI was measured every fortnight with the LAI-2000 (LI-COR Inc., Lincoln, Nebr.). Based on a previous study in a close stand (C. Vincke, personal communication), we considered a clumping factor of 0.92 and only the three inner rings of the LAI-2000 fish-eye lens, which allowed us to obtain similar estimations of LAI with direct and indirect methods. Using both types of measurements, we estimated the maximum LAI to be 5.75. The wood area index (one-sided branch area per unit ground area) was estimated to be 1.4.

Dendroecological data

During the winter 1999–2000, twenty oaks were harvested, and a stem disk was sampled on each tree at 1.3 m height. Four radii were separated from each stem disk along

the main geographical directions. The cross-sections of the radii were cut with a fine circular saw to make the anatomical structure of the wood distinguishable. Ring widths were measured along each radius, using an Addo (Addo Parker Instrument) dendrochronometer and a × 40 binocular. Ring-width series were checked and cross-dated using the COFECHA and ARSTAN softwares from the Dendrochronology Program Library (Holmes 1994). The harvested trees were used to estimate the biomass and carbon pools at stand level for different tree compartments: bark, sapwood, heartwood, bole sections, and branches of different diameter classes (André and Ponette 2003).

Climatic data

From 1996 to 2001, an automatic weather station located at Chimay in an open field (Pameseb, Libramont, Belgium) at a distance of 800 m from the stand measured precipitation (tipping bucket at 1 m height), global radiation (photovoltaic sensor solar Haeni 130 at a height of 1.5 m), air temperature (resistance sensor thermistor at 1.5 m height), and relative humidity (psychrometer thermistor at 1.5 m height). These measurements were processed hourly. Longer-term climatic data from an open field spanned the years 1954 to 2000 and came from another site in Rance located 3 km from the experimental stand (IRM, Brussels, Belgium). Long-term data were available at daily time steps and included precipitation and maximum and minimum temperature.

The MAIDEN model

General approach

The development of MAIDEN was based on the following guidelines:
(1) The model has to translate the effect of climate variability on high-resolution ecophysiological processes, but it also has to realistically describe ecosystem functioning over several decades. To reconcile these two attributes the model has a daily time step.
(2) Simple climatic variables have to be set at input of the model to be applicable at large time and spatial scales (Table 1).
(3) The model has to be applicable to different ecosystems by means of a few simple site and species parameters. At present the user has to input parameters such as altitude, latitude, absolute maximum LAI, SLA, estimated bole biomass, soil thickness, and soil textural classes (Table 1).
(4) The model should have few calibration parameters (maximum 12) to be comparable to a response function as used classically in dendroecology (Table 1).
Figure 1 provides a general overview of the model.

Climatic inputs

Climatic driving variables are daily minimum and maximum temperatures, precipitation, global radiation, and atmospheric vapor pressure deficit (Table 1). Since radiation and humidity variables are usually not available for large temporal and spatial scale applications, we coupled the MT-CLIM model (Running et al. 1987) to MAIDEN to estimate these variables from observations of daily maximum and minimum temperatures and precipitation. In MT-CLIM, humidity estimates are based on the fact that daily minimum tempera-

ture is usually very close to the dew point (Running et al. 1987). Radiation estimates are based on the fact that the diurnal temperature range is closely related to the daily mean atmospheric transmittance (Running et al. 1987; Thornton et al. 2000).

Phenology

MAIDEN simulates five phenological phases: (1) no activity in winter, (2) leaf and root expansion in spring, (3) bolewood production in summer, (4) carbohydrate reserve accumulation during early fall, and (5) leaf and root senescence during late fall. During winter (phase 1), MAIDEN does not simulate any physiological processes. Leaf and root expansion (phase 2) start when bud burst occurs. To determine the timing of bud burst, MAIDEN uses an algorithm that only considers the action of forcing temperatures. Starting on 10 February, mean degree-days are summed when mean daily temperature exceeds 5 °C, as proposed by Hoffman (1995). Then bud burst is triggered when this sum reaches a growing degree-day threshold (G_{DD}), which is a fitting parameter of the model. Leaf and root expansion (phase 2) end when LAI reaches a maximum value (L_{max}, defined below). Reserve accumulation (phase 4) starts on 1 September. Leaf and root senescence (phase 5) start when the photoperiod is less than 10 h. This phase lasts 10 days, and then winter (phase 1) is triggered again.

Radiation

Photosynthetically active radiation (PAR) is calculated from global radiation and the fraction of diffuse radiation following equations developed by Ross (1975) and Jones (1992). The transmission and absorption of PAR are calculated from Beer's law of radiation attenuation as a function of the stand LAI. The model calculates the LAI for sun leaves (LAI_{sun}) and shade leaves (LAI_{shade}) as follows:

$$[1] \quad LAI_{sun} = 1.0 - \exp(-LAI)$$

$$[2] \quad LAI_{shade} = LAI - LAI_{sun}$$

Photosynthesis

To calculate photosynthesis and stomatal conductance, MAIDEN uses an approach similar to that presented by Baldocchi (1994). The model calculates photosynthesis and stomatal conductance at leaf level, using the quadratic solution of a system of four equations and four unknowns (not presented here). This system is applied to a unit of leaf area for sun and shade leaves separately, and then photosynthesis is integrated over the whole stand canopy using the LAI of these two components. The equations for photosynthesis are adapted from Farquhar et al. (1980) to be solved at daily time steps. Thus net photosynthesis (A_n) is as follows:

$$[3] \quad A_n = [pA_{wc} + (1 - p)A_{wj}]$$

$$[4] \quad A_{wc} = W_c\left(1 - \frac{\Gamma}{c_i}\right) - R_d$$

$$[5] \quad A_{wj} = W_j\left(1 - \frac{\Gamma}{c_i}\right) - R_d$$

Table 1. MAIDEN driving variables; state variables; and site, species, and calibration parameters.

Variables and parameters	Symbol	Units
Required daily input variables		
Precipitation	P	mm
Maximum temperature	T_{max}	°C
Minimum temperature	T_{min}	°C
Optional daily input variables		
Mean global radiation	S_{rad}	W·m^{-2}
Mean daylight vapor pressure deficit	D_s	Pa
State variables		
Soil water content	θ	mm
Leaf carbon reservoir	L_c	g·m^{-2}
Bole carbon reservoir	B_c	g·m^{-2}
Root carbon reservoir	R_c	g·m^{-2}
Store carbon reservoir	S_c	g·m^{-2}
Site and species parameters		
Altitude		m
Latitude		°
Absolute maximum leaf area index	L_{max}	m^2·m^{-2}
Specific leaf area	SLA	m^2·g^{-1}
Soil layers thickness		cm
Soil textural classes		% clay, silt, sand
Calibration parameters		
Growing degree-days	G_{DD}	°C
Daily proportion of A_n limited by W_c	p	Fraction
Coefficient linking g_s to A_n[a]	a_1	—
Coefficient linking g_s to D_s[a]	D_0	Pa
Soil water stress parameter	θ_c	mm
Canopy water storage coefficient	C_{ws}	—
Temperature function coefficient for $f_{gpp \to npp}$	c_1	°C
Temperature function coefficient for $f_{npp \to store}$	c_2	°C
Root to leaf fraction	λ	—
Fraction of carbon stored to leaves and roots (phase 2)	$f_{store \to leaf/root}$	Fraction
Fraction of NPP to bole (phase 3)	$f_{npp \to bole}$	Fraction
Fraction of stored carbon to bole (phase 3)	$f_{store \to bole}$	Fraction

Note: W_c, rate of carboxylation when ribulose biphosphate is saturated; A_n, net photosynthesis; g_s, stomatal conductance; D_s, humidity deficit at leaf surface; $f_{gpp \to npp}$, fraction of gross primary production (GPP) to net primary production (NPP); $f_{npp \to store}$, fraction of NPP to store carbon.

[a]From Leuning (1995).

where A_{wc} is photosynthesis limited by the rate of carboxylation (W_c) when ribulose biphosphate is saturated, A_{wj} is photosynthesis limited by the rate of carboxylation (W_j) when ribulose biphosphate regeneration is limited by electron transport, p is a calibration parameter of the model and represents the fraction of the day when net photosynthesis is A_{wc}, Γ is the CO_2 compensation point in the absence of dark respiration, c_i is the leaf internal CO_2 concentration, and R_d is the leaf dark respiration rate. The leaf temperature is set equal to air temperature. The photosynthetic parameters and temperature corrections are from Woodrow and Berry (1980), Wullschleger (1993), Harley and Baldocchi (1995), and De Pury and Farquhar (1997). Leaf dark respiration rate (R_d) is $0.01 \times V_{max}$ (D.D. Baldocchi, personal communication). R_d is added to A_n to give the gross photosynthetic rate at leaf level (A). Stomatal conductance (g_s) is calculated using a modified version of the Leuning equation (Leuning 1995):

$$[6] \qquad g_s = g_0 + \left[\frac{a_1 A_n}{(c_s - \Gamma)[1 + (D_s/D_0)]} \right] \theta_s$$

where g_0 is the zero intercept, a_1 is an empirical coefficient, c_s is the leaf surface CO_2 concentration, D_s is the humidity deficit at the leaf surface, D_0 is an empirical coefficient reflecting the sensitivity of the stomatal conductance to D_s. The a_1 and D_s coefficients are calibration parameters of the MAIDEN model. The parameter θ_s is a soil water stress function ($0 \le \theta_s \le 1$) calculated by using the following equations:

$$[7] \qquad \theta_s = 1 - (\theta_c - \theta)/\theta_c$$

Fig. 1. Diagram showing the main features of the MAIDEN model. Processes are in italics, boxes are carbon and water pools, broken lines are links between processes, and solid lines are carbon and water fluxes.
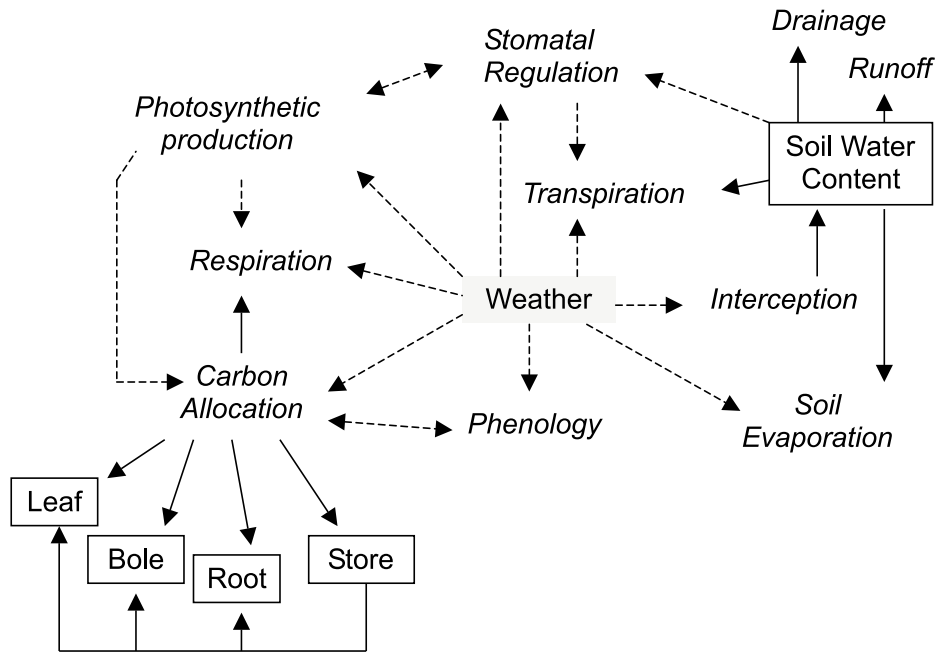
[8] $\theta_s = 1.0$ if $\theta \geq \theta_c$

where θ_c is a calibration parameter of the model, and θ is the integrated soil water content across the whole soil profile.

Water cycle

The interception model is a modification of the Gash model (Gash et al. 1995) and does not take into account stemflow, which is negligible for this stand. Daily throughfall is calculated as the sum of the incident precipitation that does not strike the canopy (direct throughfall) and the precipitation that strikes the canopy and is not re-evaporated during the day (indirect throughfall). Direct throughfall (T_d) is scaled to LAI as

[9] $T_d = \exp(-0.18\Omega_{cl}\text{LAI})P$

where Ω_{cl} is the clumping factor ($0 \leq \Omega_{cl} \leq 1$, set at 0.92), and P is the daily precipitation. $P - T_d$ is the water that strikes the canopy and fills a water reservoir to a maximum value (C_{max}) that is assumed to be proportional to stand LAI:

[10] $C_{max} = C_{ws}\text{LAI}$

where C_{ws} is a calibration parameter of the model. The water striking the canopy that is reevaporated into the atmosphere is calculated by the Penmann–Monteith equation. Canopy water that is not reevaporated falls to the ground during the night. The proportion of incident precipitation that does not reach the soil is called the interception (%).

The soil water content is computed for a series of user-defined soil layers. The net vertical flux of water between two adjacent soil horizons is computed by solving the Richard's equation for unsaturated flow. As in the Land Surface Model (Bonan 1996), MAIDEN uses a tridiagonal system of equations to solve the water balance for each layer. The relationships among the volumetric water content, the soil water potential, and the hydraulic conductivity are parameterized

according to Clapp and Hornberger (1978) and Cosby et al. (1984). The lower boundary condition for water flow (deep drainage) is free drainage. Evaporation from the soil surface, which defines the upper boundary condition, is computed using an algorithm reported by Baldocchi et al. (2000). The total soil water uptake by the trees is equal to the transpiration rate (E), which is calculated using a conductance approach:

[11] $E = g_s D_s / P_{atm}$

where P_{atm} is the atmospheric pressure. Since stomatal conductance is calculated at leaf level, E is first calculated for a unit of leaf area for sun and shade leaves and then integrated over the whole stand canopy using the LAI of these two components. In eq. 11, transpiration is limited by soil water stress through its effect on stomatal conductance.

Carbon allocation

This submodel allows MAIDEN to allocate the carbon assimilated at stand level among respiration efflux and leaf, bole, root, and store carbon reservoirs (Appendix A). The leaf, bole, root, and store reservoirs are the only carbon state variables of the model (in grams of carbon per square metre of stand). The annual increment of bole carbon reservoir at stand level, $B_{ci}(t)$, is the modeled variable that will be compared with the dendrochronological ring-width series, where t is time in year.

Most carbon-cycle modeling approaches adopt a high sensitivity of respiration to temperature (Ryan 1991). However, in the long term, plant respiration seems to acclimate to a temperature change over several days to a week (Gifford 1995). Various papers report that ecosystem CO_2 effluxes are strongly related to gross primary production (GPP), even though the exact mechanisms of such a linkage are not explicit (Gifford 1994; Waring et al. 1998; Cheng et al. 2000; Janssens et al. 2001). We combine these approaches by relat-

ing respiration to GPP, but allowing high temperature to directly influence respiration as well. Then, the following equation was used to calculate respiration (R) at stand level:

$$[12] \qquad R = kA_c[1 - \exp(-T_{max}/c_1)]$$

where k is a parameter set to 0.47 (Waring et al. 1998), A_c is stand canopy photosynthesis (equivalent to GPP), T_{max} is the maximum daily temperature, and c_1 is a calibration parameter of the model. Respiration is subtracted from GPP to give the net primary production (NPP).

To facilitate initialization of the carbon state variables, any run of the model should begin on 1 January. Then, carbon in the store reservoir (S_c) is initialized at its minimum value (400 g·m^{-2}). Initial carbon in the bole (B_c) reservoir is a user input. The maximum stand LAI for the simulation year (L_{max}) is then calculated as follows:

$$[13] \qquad L_{max} = L_{abs} \exp(-B_c/c_2)$$

where L_{abs} is the absolute maximum leaf area index for the stand (user input), and c_2 is a calibration parameter of the model. If evergreen trees are modeled, the initial leaf carbon reservoir (L_c) is calculated from L_{max} using the SLA parameter. If deciduous trees are modeled, initial L_c is set to zero. Initial root carbon (R_c) is scaled to L_{max} by an empirical coefficient (λ), which is a calibration parameter of the model:

$$[14] \qquad R_c = \lambda L_{max}/SLA$$

After initialization, the MAIDEN model partitions daily NPP and stored carbon among reservoirs according to phenological phase-dependent ratios. Extensive results in dendroecology show that stem growth is often linked from one year to the next, producing autocorrelation in tree-ring series (e.g., LeBlanc et al. 1987; Larsen and MacDonald 1995; Kahle and Spiecker 1996; Desplanque et al. 1998). In addition, results in physiology show that carbon storing occurs mainly during fall and that temperature could play an important role in this process (Larcher 1983; Kramer et al. 1991; Lacointe 2000; Lacointe et al. 1993). An original modeling procedure of carbon storing and mobilization was developed to reproduce the autocorrelation structure of tree-ring series. The equations used during each phenological phase are presented in detail in Appendix A.

During winter (phase 1) there is no activity. During leaf and root expansion (phase 2), all daily NPP is allocated to leaves and roots, as suggested by Lüdeke et al. (1994) (eqs. A1 to A4). The fraction of NPP allocated to leaves and to roots is calculated such that the ratio (λ) of leaf carbon reservoir to root carbon reservoir remains constant, λ being a calibration parameter of the model. Leaf carbon is then transformed into LAI using the SLA parameter. In addition, some carbon in the store reservoir is allocated daily to leaf and root reservoirs at a constant fraction of the amount of stored carbon ($0 \leq f_{store \to leaf/root} \leq 1$, this coefficient being a calibration parameter of the model). For deciduous trees this process is particularly important because daily NPP cannot be greater than zero if a minimal LAI does not exist. Leaf growth (phase 2) ends when LAI reaches a maximum value for the simulation year (L_{max}), which is scaled to the bole carbon reservoir on the first day of bud burst following eq. 13.

Table 2. Calibration parameters and values.

Calibration parameters	Value	Calibration data	r^2
G_{DD} (°C)	500	Bud-burst date	
p (fraction)	0.28	Transpiration	0.80
a_1	7.9	Transpiration	0.80
D_0 (Pa)	375	Transpiration	0.80
θ_c (mm)	314	Transpiration	0.80
C_{ws}	0.34	Throughfall	0.95
c_1 (°C)	30	Ring-width series	0.46
c_2 (°C)	30	Ring-width series	0.46
λ (fraction)	0.25	Ring-width series	0.46
$f_{store \to leaf/root}$ (fraction)	0.05	Ring-width series	0.46
$f_{npp \to bole}$ (fraction)	0.39	Ring-width series	0.46
$f_{store \to bole}$ (fraction)	9.0×10^{-5}	Ring-width series	0.46

Note: See Table 1 for definitions of parameters.

During bole growth (phase 3), a constant fraction of daily NPP is allocated to the bole ($0 \leq f_{npp \to bole} \leq 1$, this coefficient being a calibration parameter of the model), whereas the remaining fraction is allocated to the store reservoir (eqs. A5 to A8). The maximum size of the store reservoir is set to 1000 g·m^{-2}. In addition, a constant fraction of stored carbon remaining at the beginning of phase 2 is allocated daily to the bole reservoir ($0 \leq f_{store \to bole} \leq 1$, this coefficient being a calibration parameter of the model). The minimum size of the store reservoir is set to 400 g·m^{-2}. During the accumulation phase (phase 4), the fraction of daily NPP allocated to the store reservoir ($0 \leq f_{npp \to store} \leq 1$) is proportional to daily maximum temperature as follows:

$$[15] \qquad f_{npp \to store} = 1 - \exp(-T_{max}/c_2)$$

where T_{max} is the maximum daily temperature, and c_2 is a calibration parameter of the model. The residual NPP is allocated to the bole reservoir (eqs. A9 to A13). The leaf and root senescence period (phase 5) lasts 10 days, and root turnover is set to 20% of the root carbon reservoir existing at the end of the phase 4 (eqs. A14 to A17). Thus for deciduous trees, 10% of the leaves and 2% of the roots die each day. For evergreen trees, root turnover is modeled, but no leaf senescence takes place. Decomposition of senescent leaves and roots is not modeled.

Parameterization

The MAIDEN model was calibrated by tuning 12 parameters (Table 2). We used a simple optimization algorithm that does not involve a validation procedure on independent data, but allowed us to test the realism of the modeling schemes used at this first stage of model development. This algorithm consisted of testing successively all values of each calibration parameter separated by a constant interval inside a preselected realistic range. The set of parametric values that were retained gave the best coefficient of determination (r^2) between a measured and a simulated variable. Extensive ecophysiological data allowed us to parameterize the model sequentially using several measured variables (Table 2). Each parameter is optimized one after the other, with all other parameters being kept constant at their previous optimized values. First, the phenological data (bud-burst date) allowed us to calibrate the growing degree-day parameter

(G_{DD}, Table 2). Then, the throughfall data were used to calibrate the canopy water storage parameter (C_{ws}, Table 2). Third, soil water and transpiration data were used to calibrate four parameters, as shown in Table 2. Finally, the ring-width series was used to calibrate the six parameters related to carbon allocation (Table 2). If ecophysiological data are not available, the 12 calibration parameters of the model could possibly be estimated using ring-width series only. The MAIDEN model is written in C++® version 6.0 (Microsoft Corporation, Redmond, Wash.) and is readily available from the author.

Results

The efficiency of the MT-CLIM simulator to reproduce daily atmospheric vapor pressure (A_{vp}) and solar radiation (S_{rad}) from temperature and precipitation was tested using data collected from 1996 to 2001. We found that A_{vp} was systematically underestimated (13%), and S_{rad} was overestimated (35%). This lack of fit was corrected using a calculated linear regression between the bias (observations – simulations) and the simulations. When corrected, simulations and observations matched in a 1:1 relationship. Daily, monthly, and annual variations are quite well reproduced, and r^2 values are high for both meteorological variables (0.84 for A_{vp} and 0.78 for S_{rad}). We concluded that the MT-CLIM model could be used after corrections to estimate long-term daily and seasonal variations of atmospheric A_{vp} and S_{rad} from temperature and precipitation data at our experimental site.

Only 3 years of bud-burst date and leaf fall visual assessments were available. Then the G_{DD} parameter was calibrated by trial and error by comparing measured and simulated bud-burst dates (G_{DD} = 500 °C) (Table 2). The maximum difference between observations and estimations was 17 days, in 1998, and the minimum difference was −3 days, in 2001. The bud-burst dates over the 1960–1999 simulation period range between 23 April and 6 June, with the mean on 20 May. Leaf fall in the model was set at the end of November as estimated visually. Additional data are needed to improve the accuracy of the predictions.

The C_{ws} coefficient was set to 0.34 (C_{max} = 2.4 mm) (Table 2), a value that maximizes the r^2 (0.95) between observed and simulated throughfall (Fig. 2). Measurements and model estimations match the 1:1 relationship, with the intercept approaching zero (Fig. 2). Total measured and simulated throughfall from May to November 2001 are, respectively, 439.8 and 439.7 mm.

The MAIDEN model correctly simulates the rates of soil drying and soil rewetting from beginning of May to the end of July (Fig. 3). Heavy throughfall at the beginning of August is followed by a higher and faster rewetting in the measurements than in the simulations (Fig. 3). Rates of rewetting in September are well reproduced by the model. Globally, levels of total soil water content as well as daily and seasonal variations are well simulated (r^2 = 0.81) (Fig. 3). We concluded that the MAIDEN model could be used to simulate seasonal variations of soil water content at our experimental site.

When calibrated, the MAIDEN model satisfactorily reproduces the measurements of daily transpiration made during

Fig. 2. Modeled versus measured daily throughfall from May to November 2001. The line represents the 1:1 relationship.
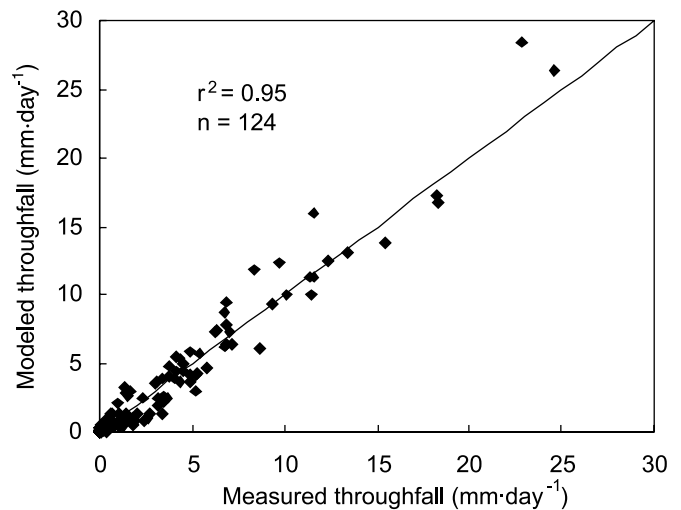
107 days (r^2 = 0.8) (Table 2 and Fig. 4). The linear regression through measured and simulated data is very near the 1:1 relationship, with the intercept approaching zero (Fig. 4). Total measured and simulated transpiration from May to November are, respectively, 102.1 and 100.6 mm. Despite this generally good fit, the model tends to slightly underestimate some of the transpiration measurements. From 8 to 15 August, measurements vary from 1.6 to 2.3 mm·day^{-1}, while simulations range from 1.1 to 1.8 mm·day^{-1}, with a mean underestimation of 25% of the observations (Fig. 4). None of the climatic inputs (temperature, radiation, relative humidity, or precipitation) reach unusual values during this period. Wind speed could explain the lack of fit because it is not inputted in the model. Nevertheless, the daily mean wind speed measured at the meteorological station is 2.05 m·s^{-1} for this period, a value that is not very high and probably does not explain the underestimation of transpiration by the model. Furthermore, the soil water stress function is 1.0 from 8 to 14 August and therefore does not reduce the simulated transpiration rates. We verified the transpiration and meteorological raw data and did not detect any measurement errors. Nevertheless, as the differences between simulations and observations are negligible in time and magnitude, we conclude that the MAIDEN model can simulate daily transpiration rates with acceptable accuracy.

When calibrating the allocation parameters on ring-width series (Table 2), the MAIDEN model predicts variations of annual bole increment, $B_{ci}(t)$, that match quite well annual variations of measured ring widths over the 1960–1999 period (Fig. 5). However, a major difference between the model and the observations occurred after the severe drought of 1976: while observations show a substantial recovery in 1977, 1978, and 1979, the model does not match these variations (Fig. 5). Furthermore, the model does not simulate the growth decline observed in 1985 and 1996. Factors other than direct climatic effects have to be taken into account to interpret the bole growth variations observed. The ability of the model to reproduce the autocorrelation structure of dendroecological series is tested in a related paper (Misson et al. 2004).

Fig. 3. Measured and modeled soil water content (left y axis) and measured daily throughfall (histogram, right y axis) from May to November 2001.
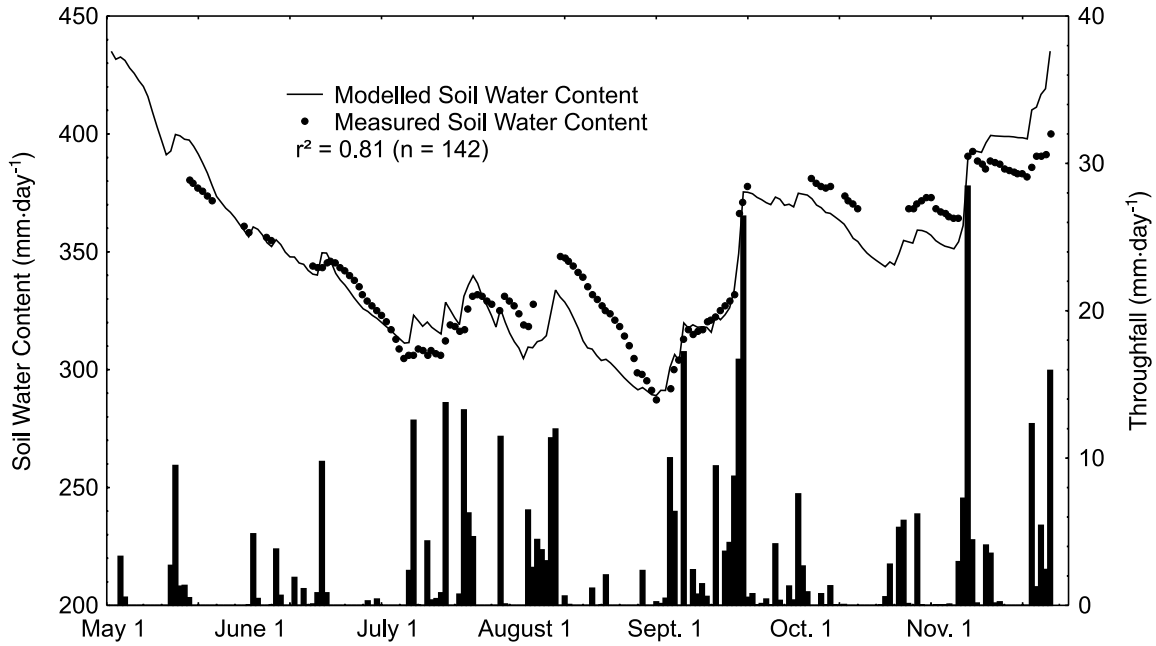
Fig. 4. Measured and modeled daily transpiration from May to November 2001. Data gaps are attributable to instrument failure or power down.
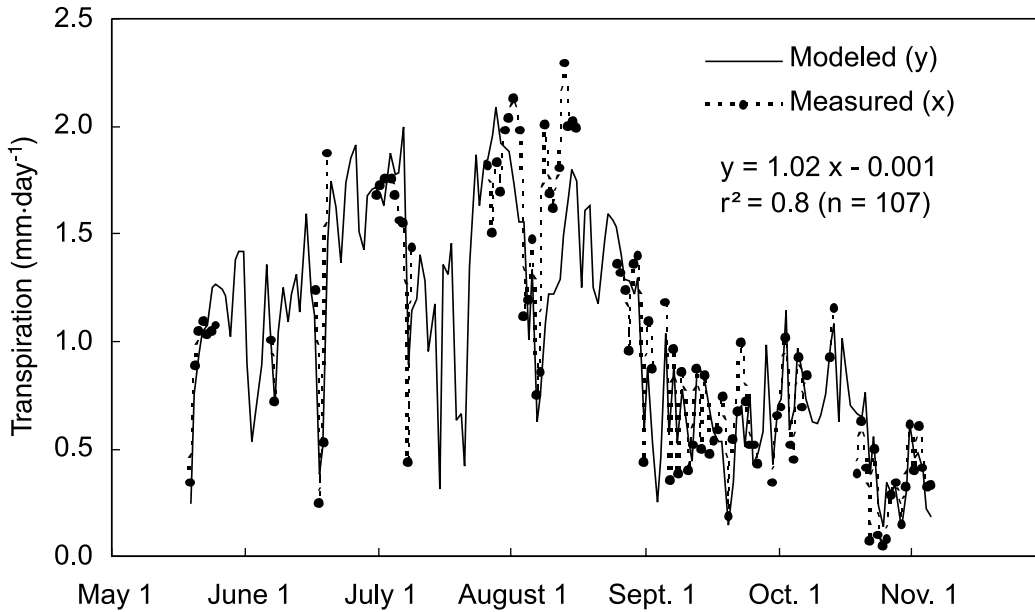
Analyses were conducted with the MAIDEN model to determine the sensitivity of transpiration to the different climatic variables. We computed the daily transpiration rates, keeping constant at their daily means, one by one, each of the input variables that control transpiration in the model (Table 3). For each of these run we computed the r^2 coefficient that, in comparison with the r^2 obtained with the normal climate data set (0.8), gives the decrease in explained variance when keeping an input variable constant. Results from the analysis show that D_s is the variable that has the most control on transpiration rates, as the r^2 coefficient decreases from 0.8 to –0.06 when this variable is kept constant

(Table 3). In contrast, transpiration seems to be relatively independent of precipitation and soil water stress (Table 3). The level of water stress during the simulation period does not drop below 0.9 when the normal climate data set is set at the input of the model. Temperature and global radiation are variables of intermediate sensitivity (Table 3).

Analyses were conducted to test the sensitivity of $B_{ci}(t)$ to the different climatic variables. When the maximum and minimum temperatures were kept at their daily means over the 1960–1999 period, r^2 was reduced from 0.44 to 0.04 (Table 3). Temperature is thus the main climatic factor that controls stem growth in this type of ecosystem, because it

Fig. 5. Measured annual ring width (left y axis) and modeled annual bole increment, $B_{ci}(t)$, (right y axis) from 1960 to 1999.
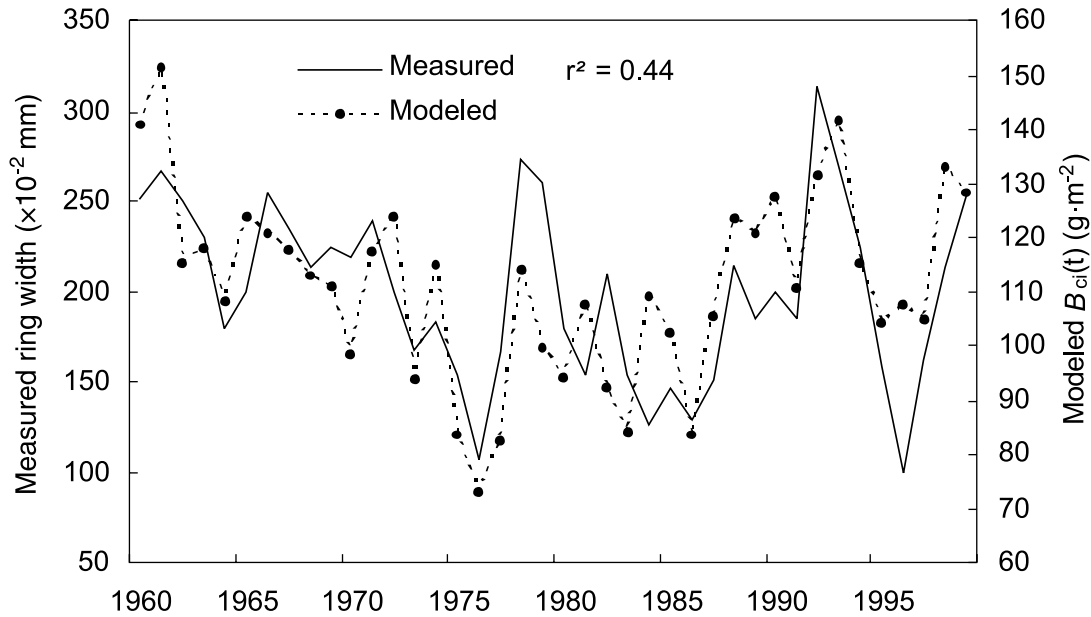
Table 3. Coefficient of determination (r^2) computed between measured and modeled transpiration and ring-width data with different climatic data sets.

Input data set	Transpiration[a]	Stem increment[b]
Normal input data set	0.80	0.44
With constant temperature	0.34	0.04
With constant precipitation and θ_s	0.76	0.44
With constant radiation	0.36	0.30
With constant vapor pressure deficit	–0.06	0.12
With constant bud-burst date		0.12

[a]Values of constant meteorological variables: maximum temperature, 18 °C; minimum temperature, 10 °C; precipitation, 3 mm and θ_s = 1.0; radiation, 200 W·m^{-2}; vapor pressure deficit, 500 Pa.

[b]Values of constant meteorological variables: maximum temperature, 12 °C; minimum temperature, 5 °C; precipitation, 2.7 mm; radiation, 220 W·m^{-2}; vapor pressure deficit, 450 Pa; bud-burst date, 1 May.

influences several major ecophysiological processes: phenology, photosynthesis, and carbon allocation. To separate the effect of temperature on annual bole growth through modeled phenological and photosynthesis – carbon allocation processes, we made a run of the model with the normal temperature data set as input, but keeping the bud-burst date constant (1 May). This run reduced the r^2 to 0.12, thus leading to the assumption that the temperature control on phenology explains the main part of interannual variance of stem increment (Table 3). By keeping daily precipitation constant, the soil water stress function remains at 1.0 all through the simulation period, and the r^2 is only marginally reduced (Table 3).

Discussion

Results show that MT-CLIM is a convenient tool for inferring unusual daily climatic variables from quite common climatic variables (precipitation, temperature) available on the large spatial and temporal scale of dendroecological studies. Nevertheless, we confirmed conclusions from previous studies that suggest that MT-CLIM should be tested more thoroughly to avoid systematic errors in the predictions (Thornton et al. 2000; Wilson et al. In press[2]). Furthermore, the daily value of temperature and precipitation are sometimes not extensively available in dendroecological studies. In cases where such data are lacking at this time step, mathematical simulators predicting daily meteorological data from monthly data may be used before MT-CLIM (Hubert et al. 1998), but this needs careful testing and validation.

The estimated a_1 parameter of the Leuning stomatal conductance model is in the range of published values (Leuning 1995) (Table 2). Nevertheless the value of D_0 is quite small. This means that transpiration is highly sensitive to variations in vapor pressure deficit (D_s), a result that is also reported in a transpiration study at a similar oak experimental site (Misson et al. 2002). In contrast, the value of θ_c is quite high, with the result that the level of water stress during the simulation period does not fall below 0.9 (see eqs. 7 and 8). The results of the parameterization process are in accordance with the sensitivity analysis, which shows that D_s is the variable that has the most control on the transpiration rates (see eqs. 6 and 11). This finding has been reported for other temperate ecosystems not limited by soil water stress (e.g., Baldocchi and Meyers 1998; Wilson et al. 2000). On other sites, there is evidence that soil water deficits control variations of canopy water exchanges (e.g., Bréda et al. 1993; Williams et al. 1996; Baldocchi 1997; Law et al. 2000b; Van Wijk et al. 2000). Adjusting the θ_c parameter in the MAIDEN model would allow soil water stress to be taken into account.

The r^2 between observed ring-width series and simulated $B_{ci}(t)$ is 0.44, which is in the range of ring-width variance explained by a dendroclimatic model in temperate ecosys-

[2]H.G. Wilson, R. Handcock, W.A. Gough, and F. Csillag. Improving the accuracy of solar radiation calculations to the boreal region. Geogr. Environ. Model. In press.

tem, where climate is not as constraining as in other conditions (Cook and Kairiukstis 1990). Mean $B_{ci}(t)$ over the simulation period is 110.5 g·m^{-2}·year^{-1} of carbon, or 2.82 m^3·ha^{-1}·year^{-1} of wood biomass. These figures are in the range of 2 to 6 m^3·ha^{-1}·year^{-1} found in the literature for such ecosystems (Hamilton and Christie 1971; Delhaise 1988). An estimation done using a biomass equation (André and Ponette 2003) coupled with carbon content analyses and a retrospective evaluation of stand density gives a value of 131.5 g·m^{-2}·year^{-1} of carbon, which is 16% higher than the simulation values. The NPP-to-GPP ratio given by the model over the simulation period is 0.37 ± 0.01 (mean ± SD), which is lower than the ratio presented in other publications (Gifford 1994, 1995; Waring et al. 1998). This indicates that NPP may be underestimated by the model. Before modifying MAIDEN, more data and tests are needed to draw inferences about the accuracy of those predictions.

As for transpiration, sensitivity analysis shows that precipitation and soil water stress are not major controlling factors of stem increment in this type of ecosystem, mainly because of high annual precipitation ($\cong$1000 mm·year^{-1}) and large soil water capacity ($\cong$600 mm). On the contrary, the spring phenological processes seem to greatly influence the interannual variance of bole increment. Previous studies found that a large part of the annual bole increment for oak occurs during the first weeks of the vegetative period (Lachaud and Bonnemain 1981; Bréda and Granier 1996). Therefore the synchronization of favorable climatic conditions could be crucial during this active period of the annual growth cycle. However, different authors have shown that latewood width remains generally larger than earlywood width in sessile oak, and that interannual variance in ring width is mostly accounted for by the variation in latewood width (Zhang 1997; Feuillat et al. 1997; Berges et al. 2000). Instead, as supported by much observational evidence, spring phenological processes are likely to exert strong control over interannual variations of bole increment through their influence on growing-season length. At the Harvard Forest, Goulden et al. (1996) found that large changes in annual gross ecosystem exchange were associated with modest changes in the timing of leaf expansion in spring. Analysis of satellite data by Myneni et al. (1997) suggested that the productivity of terrestrial vegetation in northern latitudes has increased because of a lengthening of the active growing season. Ecosystem simulation studies based on process-based models have found a good correlation between ecosystem productivity and dates of spring growth (Berninger 1997; White et al. 1999). In our case, the modeled growing-season length ranged from 147 to 191 days during the simulation period and was positively correlated with simulated $B_{ci}(t)$ (r^2 = 0.39), with a slope of 1.24 g·m^{-2}·day^{-1}. This provides evidence that phenological processes related to the timing of bud burst influence bole growth in this temperate sessile oak stand.

The model shows several inconsistencies in annual bole growth variations compared with observations. The important growth recovery after the 1976 drought stress has been observed on many sites in Europe with oak and other tree species (Spiecker 1991, 1995; Bräker 1996; Köhl et al. 1996). So far, this phenomenon has not been unambiguously interpreted. Bräker (1996) argues that some trees have declined on the stands affected by the severe 1976 weather impact, which decreased the competitive pressure on the remaining trees. Since ring-width series are individual-tree data, they integrate a competitive pressure signal, while annual bole increment modeled at stand level does not. No specific data are available to test this hypothesis at our study site. Furthermore, postdrought decline and mortality are likely to be concentrated in the competitively inferior class of trees, and their mortality probably influences the remaining trees to a small extent only. However, it is well known that silvicultural thinning operations can have a substantial influence on the radial growth of residual trees (e.g., Misson et al. 2003). Hence, to take into account the effects of stand density variations on individual bole increment in natural or managed forests, further development of the model should integrate a cohort description of the stand (Korol et al. 1991). This would enable the model to distribute the assimilated carbon at canopy level to individual trees of different sizes.

Results also show an important discrepancy between bole increment observation and simulation in 1996. The 1996 growth reduction that is not simulated by the model can be partly attributed to the spread of worm defoliation of various species that has been reported in northern France and Belgium in several studies (Hett 1997; Delbeuck 2000). Crown condition assessments in the experimental stand were made in 1996 using a standard European methodology (Eichorn 1994), and higher than usual defoliation has been attributed to infestation by *Tortrix viridina* L. in the spring (Thierron 1998).

While tree growth can be limited by soil nitrogen availability (Cole 1981), the MAIDEN model does not include a nutrient budget at the ecosystem and (or) tree level and thus does not account for the influence of nitrogen on annual tree-growth variability. Leroux et al. (2001) noticed that only a few of the 27 tree-growth models they reviewed account for tree nutrient budget, using generally crude formulations for nutrient uptake, allocation, uses, and losses. This reflects our poor understanding of the processes concerning the sources, magnitudes, and timing of available nitrogen in the soil–plant complex. Nevertheless, a linkage between carbon and nitrogen budget is clearly manifest through the dependency of photosynthetic capacity on leaf nitrogen content (e.g., Wong et al. 1985), and such a linkage has already been used in gas exchange models (Thornley 1998). Furthermore, attempts have been made to incorporate nitrogen budgets at stand level in models of forest ecosystem processes (including biomass turnover; leaf, root, and litter decomposition; nitrogen mineralization; and nitrogen allocation and loss) (Running and Gower 1991). Although these relationships have never been tested against long-term tree-growth data, they could potentially improve the fit of the MAIDEN model, especially in our experimental oak stand, where chemical analyses suggest that nitrogen may be a potentially limiting nutrient (Thierron 1998).

Conclusion

A large number of process-based tree-growth models already exists (for a review see Ceulemans 1996; Leroux et al. 2001). Upon assessing the range of existing models, we

identified key strategies for modeling ecophysiological processes on the time and spatial scale corresponding to our objectives. Thus, most parts of MAIDEN were adapted and modified from previous models. They were combined to offer an original and comprehensive tool to analyze the relationship between climate variability, ecophysiological processes, and annual tree growth. The MAIDEN model is particularly suited for analyzing dendreocological data because it uses simple species, site condition, and climatic variables as input. Furthermore, MAIDEN represents an advance in our understanding of relationships between climate and tree growth because it gives more insights into the ecophysiological processes involved than classical statistical methods. Testing the model by use of daily ecophysiological data as well as decadal tree-ring data provided a rigid test of the modeling approaches.

We presented evidence that phenological processes related to the timing of bud burst affect the length of the growing season and thus greatly influence the variability of bole growth of this temperate sessile oak stand. However, since the model is a simplification of reality, a number of processes are excluded from it, which explains why discrepancies sometimes exist between observed and simulated data. At this level as well, the model is useful because it helps identify the gaps in our knowledge and points to areas where more empirical research is needed. The model could be improved by including processes concerning the sources, magnitudes, and timing of available nitrogen in the soil–plant complex, as well as allometric relationships that would simulate the effects of thinning on ring width at individual-tree level.

Acknowledgements

References

André, F., and Ponette, Q. 2003. Comparison of biomass and nutrient content between oak (*Quercus petraea*) and hornbeam (*Carpinus betulus*) trees in a coppice-with-standards stand in Chimay (Belgium). Ann. For. Sci. **60**(6): 489–502.

Baldocchi, D.D. 1994. An analytical solution for coupled leaf photosynthesis and stomatal conductance models. Tree Physiol. **14**: 1069–1079.

Baldocchi, D.D. 1997. Measuring and modeling carbon dioxide and water vapour exchange over a temperate broad-leaved forest during the 1995 summer drought. Plant Cell. Environ. **20**: 1108–1122.

Baldocchi, D.D., and Meyers, T. 1998. On using eco-physiological, micrometeorological and biogeochemical theory to evaluate carbon dioxide, water vapour and trace gas fluxes over vegetation: a perspective. Agric. For. Meteorol. **90**: 1–25.

Baldocchi, D.D., Law, B.E., and Anthoni, P.M. 2000. On measuring and modeling energy fluxes above the floor of a homogeneous and heterogeneous conifer forest. Agric. For. Meteorol. **102**: 187–206.

Berges, L., Dupouey, J.L., and Franc, A. 2000. Long-term changes in wood density and radial growth of *Quercus petraea* Liebl. in northern France since the middle of the nineteenth century. Trees Struct. Funct. **14**: 398–408.

Berninger, F. 1997. Effects of drought and phenology on GPP in *Pinus sylvestris*: a simulation study along a geographical gradient. Funct. Ecol. **11**: 33–42.

Berninger, F., and Nikinmaa, E. 1997. Differences in pipe model parameters determine differences in growth and affect response of Scots pine to climate change. Funct. Ecol. **11**: 146–156.

Bonan, G.B. 1996. A land surface model (LSM version 1.0) for ecological, hydrological, and atmospheric studies: technical description and user's guide. National Center for Atmospheric Research, Boulder, Colo. Tech. Note NCAR/TN-417.

Bräker, O.U. 1996. Growth trends of Swiss forests: tree-ring data. Case study Toppwald. *In* Growth trends in European forests. *Edited by* H. Spiecker, K. Mielikäinen, M. Köhl, and J.P. Skovsgaard. Springer Verlag, Berlin, Germany. pp. 199–217.

Bréda, N., and Granier, A. 1996. Variations intra- et interannuelles de transpiration, LAI et croissance radiale d'un peuplement de chêne sessile. Ann. Sci. For. **53**: 521–536.

Bréda, N., Cochard, H., Dreyer, E., and Granier, A. 1993. Water transfer in a mature oak stand (*Quercus petreae*): seasonal evolution and effects of a severe drought. Can. J. For. Res. **23**: 1136–1143.

Ceulemans, R. 1996. An inventory of tree and stand growth models with potential application in short term forestry. Biomass Bioenergy, **11**: 95–107.

Cheng, W.X., Sims, D.A., and Luo, Y.Q. 2000. Photosynthesis, respiration, and net primary production of sunflower stands in ambient and elevated atmospheric CO_2 concentrations: an invariant NPP:GPP ratio? Global Change Biol. **6**: 931–941.

Clapp, R.B., and Hornberger, G.M. 1978. Empirical equations for some soil hydraulic properties. Wat. Resour. Res. **14**: 601–604.

Cole, D.W. 1981. Nitrogen uptake and translocation by forests ecosystem. Ecol. Bull. **33**: 219–232.

Cook, E.R., and Kairiukstis, L.A. 1990. Methods of dendrochronology: applications in the environmental sciences. Kluwer Academic Publisher, Dordrecht, Netherlands.

Cosby, B.J., Hornberger, G.M., Clapp, R.B., and Ginn, T.R. 1984. A statistical exploration of the relationships of soil moisture characteristics to the physical properties of soils. Water Resour. Res. **20**: 682–690.

Delbeuck, C. 2000. L'environnement wallon à l'aube du XXIème siècle : état de l'Environnement Wallon 2000. Ministère de la Région Wallonne, Namur, Belgium.

Delhaise, C. 1988. Ecostèmologie d'un bassin versant forestier : les facteurs physiques, biotiques et anthropiques. Ph.D. thesis, Université catholique de Louvain, Louvain-la-Neuve, Belgium.

De Pury, D.G.G., and Farquhar, G.D. 1997. Simple scaling of photosynthesis from leaves to canopies without the errors of big-leaf models. Plant Cell. Environ. **20**: 537–557.

Desplanque, C., Rolland, C., and Michalet, R. 1998. Dendroécologie comparée du sapin blanc (*Abies alba*) et de l'épicea commun (*Picea abies*) dans une vallée alpine de France. Can. J. For. Res. **28**: 737–748.

Eichorn, J. 1994. Visual assessment of crown conditions and submanual on visual assessment of crown condition on intensive monitoring plots. Manual on methods and criteria for harmonized sampling, assessment, monitoring and analysis of the effects of air pollution on forests. Programme Coordinating Centres of International Co-operative Programme on Assessment and Monitoring of Air Pollution Effects on Forests, Hamburg, Germany.

Farquhar, G.D., von Caemmerer, S., and Berry, J.A. 1980. A biochemical model of photosynthetic CO_2 assimilation in leaves of C3 species. Planta, **149**: 78–90.

Feuillat, F., Dupouey, J.L., and Sciama, D. 1997. A new attempt at discrimination between *Quercus petraea* and *Quercus robur* based on wood anatomy. Can. J. For. Res. **27**: 343–351.

Fritts, H.C., and Swetnam, T.W. 1989. Dendroecology: a tool for evaluating variations in past and present forest environment. Adv. Ecol. Res. **19**: 111–118.

Gash, J.H.C., Lloyd, C.R., and Lachaud, G. 1995. Estimating sparse forest rainfall interception with an analytical model. J. Hydrol. **70**: 79–86.

Gifford, R.M. 1994. The global carbon cycle: a viewpoint on the missing sink. Aust. J. Plant Physiol. **21**: 1–15.

Gifford, R.M. 1995. Whole plant respiration and photosynthesis of wheat under increased CO_2 concentration and temperature: long-term vs. short-term distinctions for modelling. Global Change Biol. **1**: 385–396.

Goulden, M.L., Munger, J.W., Fan, S.M., Daube, B.C., and Wofsy, S.C. 1996. Exchange of carbon dioxide by a deciduous forest: response to interannual climate variability. Science (Washington, D.C.), **271**: 1576–1578.

Hamilton, G.J., and Christie, J.M. 1971. Forest management tables. Forestry commission, London, UK.

Harley, P.C., and Baldocchi, D.D. 1995. Scaling carbon dioxide and water vapour exchange from leaf to canopy in a deciduous forest: leaf level parameterization. Plant Cell Environ. **18**: 1146–1156.

Hatton, T.J., Stephen, J.M., and Reece, P.H. 2000. Estimating stand transpiration in an *Eucalyptus populnea* woodland with the heat pulse method: measurement errors and sampling strategies. Tree Physiol. **15**: 219–227.

Hett, P. 1997. Les tribulations de la chenille processionnaire du chêne. Arborescences, **67**: 34–36.

Hoffman, F. 1995. FAGUS, a model for growth and development of beech. Ecol. Model. **83**: 327–348.

Holmes, R.L. 1994. Dendrochronology Program Library (DPL): user's guide. University of Arizona, Tucson, Ariz.

Hubert, B., François, L., Warnant, P., and Strivay, D. 1998. Stochastic generation of meteorological variables and effects on global models of water and carbon cycles in vegetation and soils. J. Hydrol. **212**: 318–334.

Hunt, E.R., Jr., Martin, F.C., and Running, S.W. 1991. Simulating the effect of climatic variation on stem carbon accumulation of a ponderosa pine stand: comparison with annual growth increment data. Tree Physiol. **9**: 161–172.

Janssens, I.A., Lankreijer, H., Matteucci, G., Kowalski, A.S., Buchmann, N., Epron, D., Pilegaard, K., Kutsch, W., Longdoz, B., Grunwald, T., Montagnani, L., Dore, S., Rebmann, C., Moors, E.J., Grelle, A., Rannik, U., Morgenstern, K., Oltchev, S., Clement, R., Gudmundsson, J., Minerbi, S., Berbigier, P., Ibrom, A., Moncrieff, J., Aubinet, M., Bernhofer, C., Jensen, N.O., Vesala, T., Granier, A., Schulze, E.D., Lindroth, A., Dolman, A.J., Jarvis, P.G., Ceulemans, R., and Valentini, R. 2001. Productivity overshadows temperature in determining soil and ecosystem respiration across European forests. Global Change Biol. **7**: 269–278.

Jones, H.G. 1992. Plants and microclimate. Cambridge University Press, Cambridge, UK.

Kahle, H.P., and Spiecker, H. 1996. Adaptability of radial growth of Norway spruce to climate variations: results of a site-specific dendroecological study in high elevations of the black forest (Germany). *In* Tree rings, environment, and humanity. *Edited by*

J.S. Dean, D.M. Meko, and T.W. Swetnam. University of Arizona, Tucson, Ariz. pp. 785–801.

Köhl, M., Zingg, A., and Bräker, O.U. 1996. A comparison of analytical approaches for detecting diameter growth trends: case studies from Switzerland. *In* Growth trends in European forests. *Edited by* H. Spiecker, K. Mielikäinen, M. Köhl, and J.P. Skovsgaard. Springer Verlag, Berlin, Germany. pp. 267–274.

Korol, R.L., Running, S.W., Milner, K.S., and Hunt, E.R. 1991. Testing a mechanistic carbon balance model against observed tree growth. Can. J. For. Res. **21**: 1098–1105.

Kramer, P.J., Kozlowski, T.T., and Pallardy, S.G. 1991. The physiological ecology of woody plants. Academic Press Inc., San Diego, Calif.

Lachaud, S., and Bonnemain, J.-L. 1981. Xylogénèse chez les dicotylédones arborescentes. I. Modalités de la remise en activité du cambium et de la xylogénèse chez les hêtres et les chênes âgés. Can. J. Bot. **59**: 1222–1230.

Lacointe, A. 2000. Carbon allocation among tree organs: a review of basic processes and representation in functional–structural tree models. Ann. For. Sci. **57**: 521–533.

Lacointe, A., Kajji, A., Améglio, T., Daudet, F.A., Cruiziat, P., Archer, P., and Frossard, J.S. 1993. Mobilization of carbon reserves in young walnut trees. Acta Bot. Gall. **4**: 435–441.

Larcher, W. 1983. Physiological plant ecology. Springer Verlag, Berlin, Germany.

Larsen, C.P.S., and MacDonald, G.M. 1995. Relation between tree-ring widths, climate, and annual area burned in the boreal forest of Alberta. Can. J. For. Res. **25**: 1746–1755.

Law, B.E., Waring, R.H., Anthoni, P.M., and Aber, J. 2000*a*. Measurements of gross and net ecosystem productivity and water vapour exchange of a *Pinus ponderosa* ecosystem, and an evaluation of two generalized models. Global Change Biol. **6**: 155–168.

Law, B.E., Williams, M., Anthoni, P., Baldocchi, D.D., and Unsworth, M.H. 2000*b*. Measuring and modeling seasonal variation of carbon dioxide and water vapour exchange of a *Pinus ponderosa* forest subject to soil water deficit. Global Change Biol. **6**: 613–630.

LeBlanc, D.C., and Foster, R.F. 1992. Predicting effects of global warming on growth and mortality of upland oak species in the midwestern United States: a physiologically based dendroecological approach. Can. J. For. Res. **22**: 1739–1752.

LeBlanc, D.C., and Terrel, M. 2001. Dendroclimatic analyses using Thornthwaite–Mather-type evapotranspiration models: a bridge between dendroecology and forest simulation models. Tree-Ring Res. **57**: 55–66.

LeBlanc, D.C., Raynal, D.J., and White, E.H. 1987. Acidic deposition and tree growth: II. Assessing the role of climate in recent growth declines. J. Environ. Qual. **16**: 334–340.

Leroux, X., Lacointe, A., Escobar-Gutiérrez, A., and Le Dizès, S. 2001. Carbon-based models of individual tree growth: a critical appraisal. Ann. For. Sci. **58**: 469–506.

Leuning, R. 1995. A critical appraisal of a combined stomatal-photosynthesis model for C3 plants. Plant Cell Environ. **18**: 339–355.

Lüdeke, M.K.B., Badeck, F.W., Otto, R.D., Häger, C., Dönges, S., Kindermann, J., Würth, G., Lang, T., Jäkel, U., Klaudius, A., Ramge, P., Habermehl, S., and Kohlmaier, G.H. 1994. The Frankfurt biosphere model: a global process-oriented model of seasonal and long-term CO_2 exchange between terrestrial ecosystems and the atmosphere. I. Model description and illustrative results for cold deciduous and boreal forests. Clim. Res. **4**: 143–166.

Mäkelä, A., and Hari, P. 1986. Stand growth-model based on carbon uptake and allocation in individual trees. Ecol. Model. **33**: 205–229.

Misson, L., Rasse, D.P., Vincke, C., Aubinet, M., and François, L. 2002. Predicting transpiration from forest stands in Belgium for the 21st century. Agric. For. Meteorol. **111**: 265–282.

Misson, L., Vincke, C., and Devillez, F. 2003. Frequency responses of radial growth series after different thinning intensities in Norway spruce (*Picea abies* (L.) Karst.) stands. For. Ecol. Manage. **177**: 51–63.

Misson, L., Rathgeber, C., Nicault, A., and Guiot, J. 2004. Dendroecological analysis of climatic effects on *Quercus petreae* and *Pinus halepensis* radial growth using the process-based MAIDEN model. Can. J. For. Res. **34**: 888–898.

Myneni, R.B., Keeling, C.D., Tucker, C.J., Asrar, G., and Nemani, R.R. 1997. Increased plant growth in the northern high latitudes from 1981 to 1991. Nature (London), **386**: 698–702.

Preushler, T. 1994. Phenological observations. Manual on methods and criteria for harmonized sampling, assessment, monitoring and analysis of the effects of air pollution on forests. Programme Coordinating Centres of International Co-operative Programme on Assessment and Monitoring of Air Pollution Effects on Forests, Hamburg, Germany.

Rathgeber, C., Nicault, A., Guiot, J., Keller, T., Guibal, F., and Roche, P. 2000. Simulated responses of *Pinus halepensis* forest productivity to climatic change and CO_2 increase using a statistical model. Global Planet. Change, **26**: 405–421.

Ross, J. 1975. Radiative transfer in plant communities. Vegetation and atmosphere. Vol. 1. Principles. Academic Press, New York.

Running, S.W., and Coughlan, J.C. 1988. A general model of forest ecosystem processes for regional applications I. Hydrologic balance, canopy gas exchange and primary production processes. Ecol. Model. **42**: 125–154.

Running, S.W., and Gower, S.T. 1991. Forest-BGC, A general-model of forest ecosystem processes for regional applications. 2. Dynamic carbon allocation and nitrogen budgets. Tree Physiol. **9**: 147–160.

Running, S.W., Nemani, R.R., and Hungerford, R.D. 1987. Extrapolation of synoptic meteorological data in mountainous terrain and its use for simulating forest evapotranspiration and photosynthesis. Can. J. For. Res. **17**: 472–483.

Ryan, M.G. 1991. Effects of climate change on plant respiration. Ecol. Appl. **1**: 157–167.

Spiecker, H. 1991. Growth variation and environmental stresses: long-term observations on permanent research plots in Southwestern Germany. Water Air Soil Pollut. **54**: 247–256.

Spiecker, H. 1995. Growth dynamics in a changing environment — long-term observations. Plant Soil, **168**: 555–561.

Thierron, V. 1998. Installation de huit placettes permanentes de surveillance intensive d'écosystèmes forestiers en région wallonne. Rapport final. Unité des eaux et forets, Université catholique de Louvain, Louvain-la-Neuve, Belgium.

Thornley, J.H.M. 1998. Dynamic model of leaf photosynthesis with acclimation to light and nitrogen. Ann. Bot. **81**: 421–430.

Thornton, P.E., Hasenauer, H., and White, M.A. 2000. Simultaneous estimation of daily solar radiation and humidity from observed temperature and precipitation: an application over complex terrain in Austria. Agric. For. Meteorol. **104**: 255–271.

Vaganov, E.A. 1996. Analyses of seasonal tree-ring formation and modeling in dendrochronology. *In* Tree rings, environment, and humanity. *Edited by* J.S. Dean, D.M. Meko, and T.W. Swetnam. University of Arizona, Tucson, Ariz. pp. 73–87.

Van Wijk, M.T., Dekker, S.C., Bouten, W., Bosveld, F.C., Kohsiek, W., Kramer, K., and Mohren, G.M.J. 2000. Modeling daily gas exchange of a Douglas-fir forest: comparison of three stomatal conductance models with and without a soil water stress function. Tree Physiol. **20**: 115–122.

Waring, R.H., Landsberg, J.J., and Wiliams, M. 1998. Net primary production of forests: a constant fraction of gross primary production. Tree Physiol. **18**: 129–134.

White, M.A., Running, S.W., and Thornton, P.E. 1999. The impact of growing-season length variability on carbon assimilation and evapotranspiration over 88 years in the eastern US deciduous forest. Int. J. Biometeorol. **42**: 139–145.

Williams, M., Rastetter, E.B., Fernandes, D.N., Goulden, M.L., Wofsy, S.C., Shaver, G.R., Melillo, J.M., Munger, J.W., Fan, S.-M., and Nadelhoffer, K.J. 1996. Modelling the soil–plant–atmosphere continuum in a *Quercus–Acer* stand at Harvard Forest: the regulation of stomatal conductance by light, nitrogen and soil/plant hydraulic properties. Plant Cell Environ. **19**: 911–927.

Wilson, K.B., Baldocchi, D.D., and Hanson, P.J. 2000. Quantifying stomatal and non-stomatal limitations to carbon assimilation resulting from leaf aging and drought in mature deciduous tree species. Tree Physiol. **20**: 787–797.

Wong, S.C., Cowan, I.R., and Farquhar, G.D. 1985. Leaf conductance in relation to rate of CO_2 assimilation 1. Influence of nitrogen nutrition, phosphorous-nutrition, photon flux-density, and ambient partial-pressure of CO_2 during ontogeny. Plant Physiol. **78**: 821–825.

Woodrow, I.E., and Berry, J.A. 1980. Enzymatic regulation of photosynthetic CO_2 fixation in C3 plants. Annu. Rev. Plant Physiol. Plant Mol. Biol. **39**: 533–594.

Woodward, F.I., and Smith, T.M. 2001. Impact of climate and CO_2 on the terrestrial carbon cycle. *In* The carbon cycle. *Edited by* T.M.L. Wigley and D.S. Schimel. Cambridge University Press, Cambridge, UK. pp. 248–257.

Wullschleger, S.D. 1993. Biochemical limitations to carbon assimilation in C3 plants. A retrospective analysis of the A/Ci curves from 109 species. J. Exp. Bot. **44**: 907–920.

Zhang, S.Y. 1997. Variations and correlations of various ring width and ring density features in European oak: implications in dendroclimatology. Wood Sci. Technol. **31**: 63–72.

Appendix A. The allocation submodel.

The model partitions daily net primary production and stored carbon between carbon reservoirs according to phenological phase-dependent ratios. Table A1 lists the symbols, units, and definitions. Table A2 lists the equations.

Table A1. Symbols, units, and definitions used in the allocation submodel equations.

Symbol	Units	Definition
NPP	$g \cdot m^{-2} \cdot day^{-1}$	Net primary production
λ	Fraction	Leaf/root ratio
$L_{c,i}$	$g \cdot m^{-2}$	Carbon in leaf reservoir (L_c) at the ith day of the run
$B_{c,i}$	$g \cdot m^{-2}$	Carbon in bole reservoir (B_c) at the ith day of the run
$R_{c,i}$	$g \cdot m^{-2}$	Carbon in root reservoir (R_c) at the ith day of the run
$S_{c,i}$	$g \cdot m^{-2}$	Carbon in store reservoir (S_c) at the ith day of the run
$f_{store \rightarrow leaf/root}$	Fraction	Fraction of stored carbon to leaves and roots (phase 2)
$f_{npp \rightarrow bole}$	Fraction	Fraction of NPP to bole (phase 3)
$f_{store \rightarrow bole}$	Fraction	Fraction of stored carbon to bole (phase 3)
$f_{npp \rightarrow store}$	Fraction	Fraction of NPP to the store reservoir (phase 4)
T_{max}	°C	Maximum daily temperature

Table A2. Equations used in the allocation submodel.

Phase	Equation	Equation No.
Winter (phase 1)	No activity	
Spring (phase 2)	$L_{c,i} = L_{c,i-1} + \dfrac{L_c}{L_c + R_c}(\text{NPP} + f_{store \rightarrow leaf/root} S_{c,i-1})$	A1
	$B_{c,i} = B_{c,i-1}$	A2
	$R_{c,i} = R_{c,i-1} + \left(1 - \dfrac{L_c}{L_c + R_c}\right)(\text{NPP} + f_{store \rightarrow leaf/root} S_{c,i-1})$	A3
	$S_{c,i} = S_{c,i-1} - (f_{store \rightarrow leaf/root})S_{c,i-1}$ and $S_{c,i} \geq 400 \ g \cdot m^{-2}$	A4
Summer (phase 3)	$L_{c,i} = L_{c,i-1}$	A5
	$B_{c,i} = B_{c,i-1} + f_{npp \rightarrow bole} \text{NPP} + f_{store \rightarrow bole} S_{c,i-1}$	A6
	$R_{c,i} = R_{c,i-1}$	A7
	$S_{c,i} = S_{c,i-1} + (1 - f_{npp \rightarrow bole})\text{NPP} - f_{store \rightarrow bole} S_{c,i-1}$ with $S_{c,i} \geq 400 \ g \cdot m^{-2}$ and $S_{c,i} \leq 1000 \ g \cdot m^{-2}$	A8
Early fall (phase 4)	$f_{npp \rightarrow store} = 1 - \exp(-T_{max}/c_2)$	A9
	$L_{c,i} = L_{c,i-1}$	A10
	$B_{c,i} = B_{c,i-1} + (1 - f_{npp \rightarrow store})\text{NPP}$	A11
	$R_{c,i} = R_{c,i-1}$	A12
	$S_{c,i} = S_{c,i-1} + (f_{npp \rightarrow store})\text{NPP}$	A13
Late fall (phase 5)	$L_{c,i} = L_{c,i-1} - 0.1 L_{c,i-1}$	A14
	$B_{c,i} = B_{c,i-1}$	A15
	$R_{c,i} = R_{c,i-1} - 0.02 R_{c,i-1}$	A16
	$S_{c,i} = S_{c,i-1}$	A17